Journal of Materials Chemistry B

PAPER

Cite this: J. Mater. Chem. B, 2018, 6, 6637

Imaging of intracellular sulfane sulfur expression changes under hypoxic stress *via* a selenium-containing near-infrared fluorescent probe†

Min Gao,‡[ab] Rui Wang,‡[ac] Fabiao Yu,*[ac] Bowei Li[a] and Lingxin Chen*[ad]

Received 10th July 2018,
Accepted 19th September 2018

DOI: 10.1039/c8tb01794h

rsc.li/materials-b

Hypoxia is a significant global issue affecting the health of organisms. Oxygen homeostasis is critical for mammalian cell survival and cellular activities. Hypoxic stress can lead to cell injury and death, which contributes to many diseases. Sulfane sulfur is involved in crucial roles in physiological processes of maintaining intracellular redox state and ameliorating oxidative damage. Therefore, real-time imaging of changes in sulfane sulfur levels is important for understanding their biofunctions in cells. In this study, we develop a new near-infrared (NIR) fluorescent probe BD-diSeH for imaging of sulfane sulfur changes in cells and *in vivo* under hypoxic stress. The probe includes two moieties: an NIR azo-BODIPY fluorophore equipped with a strong nucleophilic phenylselenol group (–SeH). The probe is capable of tracing dynamic changes of endogenous sulfane sulfur based on a fast and spontaneous intramolecular cyclization reaction. The probe has been successfully used for imaging sulfane sulfur in 3D-multicellular spheroid and mouse hippocampus under hypoxic stress. The overall levels of sulfane sulfur are affected by the degree and length of hypoxic stress. The results reveal a close relationship between sulfane sulfur and hypoxia in living cells and *in vivo*, allowing better understanding of physiological and pathological processes involving sulfane sulfur. Moreover, to investigate the effects of environmental hypoxia on aquatic animals, this probe has been applied for sulfane sulfur detection in hypoxic zebrafish.

Introduction

Hypoxia is now a pressing global environmental problem, which leads to deleterious ecological effects; therefore, it has received increasing scientific attention. Due to rapid industrialization and human population growth, its severity is likely to be exacerbated.[1,2] Since oxygen is necessary for supporting normal physiological activities and survival of general organisms, hypoxia can disrupt highly sophisticated, programmed processes in normal histogenesis and organogenesis and ultimately threaten the survival and health of organisms.[3] *In vitro* and *in vivo* studies show that hypoxic stress can induce a normal physiological response to imbalance in oxygen supply, trigger a burst of reactive oxygen species (ROS) in cells, and finally induce cell apoptosis. To prevent these damages, cells' own intricate antioxidant regulatory systems balance redox homeostasis. Reactive sulfur species (RSS) in biological systems are sulfur-containing molecules, which act as regulators of intracellular redox states and prevent apoptosis.[4,5] RSS include disulfide-*S*-oxides, sulfenic acids, thiyl radicals, thiols, disulfide, hydrogen sulfide, persulfides, polysulfides and other inorganic sulfur derivatives. These species have attracted increasing attention in physiological research.[6–9] Therefore, detecting the changes in reactive species is useful for better understanding the effects of hypoxia on organisms.

Sulfane sulfur belongs to RSS, and it contains a reactive sulfur atom with six valence electrons but no charge (represented as S^0).[10] Biologically, sulfane sulfur is generally present as persulfides (RSSH), hydrogen polysulfides (H_2S_n, $n \geq 2$), polysulfides (R–S_n–R, $n \geq 3$) and protein-bound elemental sulfur (S_8). Sulfane sulfur also plays antioxidative roles in carcinogenesis and the activity of immune cells through regulation of certain enzymes.[11,12] Moreover, H_2S and sulfane sulfur have a redox partnership and coexist in biological systems. From this reactivity point-of-view, sulfane sulfur seems much more effective than H_2S in protein *S*-sulfhydration. Accumulating evidence

[a] CAS Key Laboratory of Coastal Environmental Processes and Ecological Remediation, Yantai Institute of Coastal Zone Research, Chinese Academy of Sciences, Yantai 264003, China. E-mail: lxchen@yic.ac.cn
[b] University of Chinese Academy of Sciences, Beijing 100049, China
[c] Institute of Functional Materials and Molecular Imaging, College of Emergency and Trauma, Hainan Medical University, Haikou, 571199, China. E-mail: fbyu@yic.ac.cn
[d] College of Chemistry and Chemical Engineering, Qufu Normal University, Qufu 273165, China

† Electronic supplementary information (ESI) available: Chemical synthesis and characterization of compounds, supplementary experiments, and data. See DOI: 10.1039/c8tb01794h

‡ These authors contributed equally.

indicates that the actual signaling molecule may be sulfane sulfur rather than H_2S. Currently, few methods have been developed for sulfane sulfur detection as it is highly reactive and has labile chemical properties. It is difficult to extract sulfane sulfur from living cells in real time. As is known, thiosulfoxide tautomers exist alongside sulfane sulfur (Scheme 2). The most popular spectrophotometric assay for sulfane sulfur detection depends on the nucleophilic reaction with cyanide ions to generate thiocyanate, which coordinates with Fe^{3+} to yield a red complex.[13] Unfortunately, this method requires complex processing of biological samples, which does not meet the requirements for real time and *in situ* detection. Therefore, it is challenging to accurately quantify trace amounts of sulfane sulfur in living cells and *in vivo*.

Fluorescence imaging exhibits various advantages for intracellular reactive species detection, providing greater sensitivity, excellent selectivity, convenience, less invasiveness and real-time imaging.[7,14–18] Despite rapid progress in the development of fluorescent probes for biothiol detection, such as H_2S and glutathione,[7,19–22] fluorescent probes for sulfane sulfur detection in cells still need to be developed.[23–27] Many fluorescent probes have been reported for sensitive and selective detection of H_2S_n sulfane sulfur.[28–38] Among them, Xian's group reported a series of fluorescent probes based on the nucleophilic property of H_2S_n. Our group further proposed two fluorescent probes for crosstalk research between H_2S_n and superoxide anion.[28,33] Moreover, we investigated another species of sulfane sulfur, cysteine hydropersulfide (Cys-SSH), in living cells and *in vivo* based on a ratiometric NIR fluorescent probe.[39] We suppose that the overall levels of intracellular sulfane sulfur can be associated with various physiological and pathological processes. Unfortunately, only a few fluorescent probes have been designed for sulfane sulfur detection.[25] Of particular interest are fluorescent probes that emit in the near-infrared (NIR) region, where biological autofluorescence exists minimally, to allow tissue penetration for several centimeters.[40–43] Therefore, we strove to develop a fluorescent probe that features NIR absorption and emission for overall levels of sulfane sulfur detection in cells and *in vivo*.

Herein, we designed an NIR fluorescent probe BD-diSeH, which integrated 2-hydroselenobenzoate fragments with NIR azo-BODIPY fluorophore, for the detection of sulfane sulfur in living cells and *in vivo* under hypoxic condition. BD-diSeH exhibited excellent selectivity and high sensitivity for the detection of sulfane sulfur. The relationship between the changes in sulfane sulfur and the degree and time of hypoxic stress was investigated in cells, 3D-multicellular spheroids, hippocampus and *in vivo*; the results clearly showed that the changes in sulfane sulfur under hypoxic condition can elucidate the physiological and pathological processes mediated by sulfane sulfur.

Experimental

Synthesis and characterization of BD-diSeH

2,2′-Diselanediyldibenzoic acid (80.03 mg, 0.2 mmol), azo-BODIPY (53.0 mg, 0.1 mmol), 1-ethyl-3-(3-dimethylaminopropyl)-carbodiimide hydrochloride (EDC, 38.4 mg, 0.2 mmol) and 4-dimethylaminopyridine (DMAP, 2.44 mg, 0.02 mmol) in CH_2Cl_2 (50 mL) were stirred for 12 hours at 25 °C. Then, the mixture was neutralized with dilute HBr and extracted with CH_2Cl_2. Then, the organic phase was separated and evaporated to dryness, and the resulting residue was subjected to column chromatography and eluted with CH_2Cl_2 for purification. The product (64.8 mg, 0.05 mmol) and sodium borohydride (37.8 mg, 1 mmol) were reacted for 6 h in ethanol (30 mL) under Ar atmosphere at 25 °C. Then, the mixture was partitioned between CH_2Cl_2 and H_2O. The organic layer was separated and dried over Na_2SO_4. The crude product of BD-diSeH was purified by column chromatography (eluted with CH_2Cl_2). The product was obtained as dark green crystals. Yield: 37.4 mg, 41.7%. ^{1}H NMR (500 MHz, $CDCl_3$-D_1) δ (ppm): 8.16–8.14 (m, 8H), 8.08–8.07 (m, 5H), 7.52–7.43 (m, 11H), 7.38–7.36 (m, 4H), 1.26 (s, 2H). ^{13}C NMR (125 MHz, $CDCl_3$-D_1) δ (ppm): 163.88, 161.33, 158.49, 152.82, 145.70, 144.40, 141.41, 140.41, 132.20, 131.89, 131.63, 131.21, 131.18, 131.15, 129.67, 129.43, 129.39, 129.32, 129.07, 128.69, 127.75, 127.10, 121.94, 119.11. LC-MS (ESI^-): $C_{46}H_{30}BF_2N_3O_4Se_2$ calcd 897.0628, found $[M + K^+]$ 934.0129.

Cell culture and confocal imaging

Human neuroblastoma (SH-Sy5y) cells, mouse macrophage (RAW 264.7) cells, human lung carcinoma (A549) cells, human cervical carcinoma (Hela) cells, human embryonic kidney 293 (HEK 293) cells, human hepatocellular liver carcinoma (HepG2) cells, and human hepatocellular liver carcinoma (SMMC7721) cells were obtained from the cell bank of the Shanghai Institute of Biochemistry and Cell Biology (Shanghai, China). A549 cells, RAW 264.7 cells, SMMC7721 cells, and SH-Sy5y cells were cultured in RPMI 1640 medium supplemented with 10% fetal bovine serum (FBS) at 37 °C in a humidified atmosphere containing 5% CO_2. Hela cells and HepG2 cells were cultured in DMEM medium supplemented with 10% FBS at 37 °C in a humidified atmosphere containing 5% CO_2. HEK 293 cells were cultured in MEM medium supplemented with 10% fetal bovine serum (FBS) at 37 °C in a humidified atmosphere containing 5% CO_2. Fluorescent images were acquired on an Olympus FluoView FV1000 confocal laser-scanning microscope (Japan) with an objective lens (×60). The excitation wavelength was 635 nm. Cell imaging was carried out after cells were washed with PBS three times.

Hypoxic conditions in cell incubation

Here, 0.1% O_2 concentration was generated with an AnaeroPack™ (Mitsubishi Gas Chemical Company, Inc., Japan). Also, 1–20% O_2 concentration was generated with a multi gas incubator (Sanyo) by means of N_2 substitution.

Formation of SH-SY5Y multicellular spheroids

SH-SY5Y multicellular spheroids (MCs) were cultured in low attachment multi-well plates (Corning® Costar® Ultra). MCs with diameters of 300–400 nm were chosen and incubated with BD-diSeH (1 μM) for 8 h at 37 °C. Then, MCs were washed with PBS and observed with confocal laser scanning microscopy.

Results and discussion

Design strategy for probe BD-diSeH

It seems that an NIR fluorescent probe can exhibit rapid and sensitive detection of sulfane sulfur in living cells and *in vivo*. To achieve our design strategy, a BODIPY platform was particularly selected as a fluorophore due to its high molar absorption coefficient and fluorescence quantum yield.[44] Sulfane sulfur is reactive and labile and commonly associated with its thiosulfoxide tautomers. This chemical property provides a highly reactive site, where a sulfur atom in thiosulfoxide can be readily removed by a nucleophilic group such as CN^- (Scheme 2). With this inspiration, we suggested that the selenol group (–SeH) in phenylselenol (pK_a 5.9) can be a better nucleophilic group than the mercapto group (–SH) in thiophenol (pK_a 6.5).[25] The strong nucleophilicity of –SeH can benefit the selectivity, sensitivity, and kinetics of a probe for sulfane sulfur detection.[45] The probe BD-diSeH was devised by incorporating two sulfane sulfur-responsive trigger 2-hydroselenobenzoate-containing –SeH sub-moieties into a BODIPY platform *via* an ester bridge (Scheme 2). In the presence of sulfane sulfur, the –SeH group captured a sulfur atom from thiosulfoxide, affording a reactive intermediate (BD-diSeSH), followed by an intramolecular nucleophilic attack on the ester bridge. Finally, the fluorophore was released. Detailed synthetic protocols are displayed in Scheme 1.

Spectral properties of probe BD-diSeH

To demonstrate the efficiency of BD-diSeH for measuring sulfane sulfur, the absorption and fluorescence spectra of BD-diSeH (10 μM) were examined under simulated physiological conditions (10 mM HEPES, pH 7.4, 20% fetal bovine serum). As shown in Fig. 1a, BD-diSeH exhibited an absorption peak centered at 702 nm (ε_{702nm} = 2.98 × 10^5 cm^{-1} M^{-1}). The quantum yield of BD-diSeH was determined to 0.002. After reaction with Na_2S_4 as the model source of sulfane sulfur for the following tests, a new absorption peak appeared at 707 nm (ε_{707nm} = 3.74 × 10^5 cm^{-1} M^{-1}), which indicated that BD-diSeH reacted with sulfane sulfur and released the fluorophore. Upon addition of different concentrations of Na_2S_4 (0–20 μM) to the buffer solution containing 10 μM BD-diSeH, fluorescence intensity gradually increased in the NIR region with increasing concentrations of sulfane sulfur (Fig. 1b). The fluorescence intensity at 737 nm was linearly related to the concentration of sulfane sulfur within the given range (Fig. 1c). The regression equation was $F_{\lambda_{ex/em}(707/737\,nm)}$ = 3.32 × 10^5 [Na_2S_4] + 4.59 × 10^3 with r = 0.9936. The limit of detection was determined to be 2.3 nM ($3\sigma/\kappa$) under

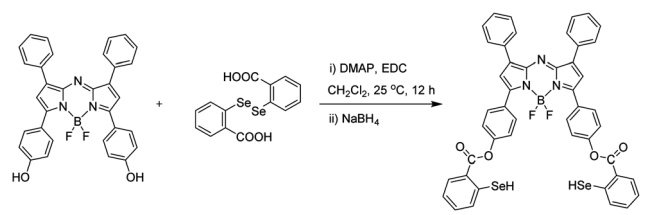

Scheme 1 Synthesis route for BD-diSeH.

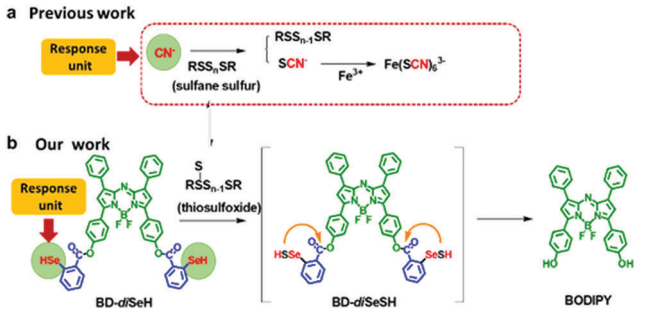

Scheme 2 Design strategy and proposed detection mechanism of BD-diSeH towards sulfane sulfur.

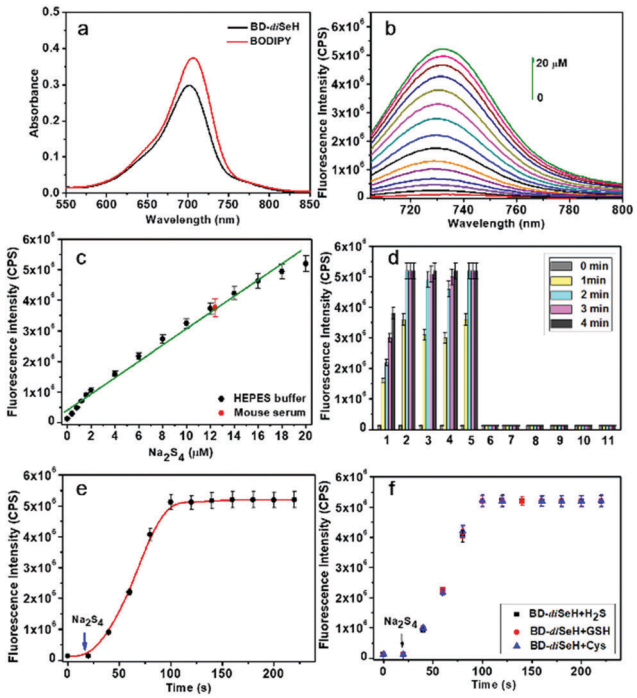

Fig. 1 (a) UV-vis absorption spectra of BD-diSeH (10 μM) before and after treatment with Na_2S_4 (20 μM). (b) Fluorescence spectra of BD-diSeH (10 μM) upon addition of Na_2S_4 (0–20 μM). Spectra were obtained after incubation of probe with Na_2S_4 for 5 min. (c) The corresponding linear relationship between fluorescence intensity and Na_2S_4 concentration (0–20 μM) in buffer solution. The red point is the mean fluorescence intensity of mouse serum. (d) Time-dependent enhancement in fluorescence response of BD-diSeH (10 μM) toward various RSS. (1) Na_2S_2, 20 μM; (2) Na_2S_4, 20 μM; (3) $PhCH_2S_4CH_2Ph$, 20 μM; (4) Cys-polysulfide, 20 μM; (5) S_8, 20 μM; (6) NaHS, 100 μM, (7) GSH, 1 mM, (8) Cys, 500 μM, (9) Hcys, 500 μM, (10) Cys–Cys, 500 μM, (11) GSSG, 500 μM. Bars represent fluorescence intensity at 0, 1, 2, 3, and 4 min after addition of various RSS. (e) Time-dependent fluorescence changes of BD-diSeH upon addition of Na_2S_4 (20 μM). (f) Time-dependent fluorescence changes of BD-diSeH upon addition of Na_2S_4 (20 μM) in the presence of interfering thiols H_2S, GSH and Cys (1 mM). All spectra were acquired in 10 mM HEPES (20% fetal bovine serum, v/v, pH 7.4). $\lambda_{ex/em}$ = 707/737 nm.

experimental conditions, which indicated that the probe had high sensitivity for the detection of sulfane sulfur. To verify whether the probe was suitable for physiological detection, the effect of pH on the probe was investigated. These results

indicated that BD-diSeH could work effectively at pH 7.4 (Fig. S1, ESI†). Since our probe could detect sulfane sulfur quantitatively under simulated physiological conditions, next, we directly tested the concentration of sulfane sulfur in BALB/c mouse serum using BD-diSeH (10 μM). The concentration of sulfane sulfur in mouse serum reached 12.4 ± 2.5 μM (the red point in Fig. 1c). The results demonstrated that our probe could qualitatively and quantitatively detect sulfane sulfur in biological samples.

Selectivity

Fluorescence probes must offer rapid and selective responses to sulfane sulfur because it undergoes rapid metabolism in biological systems. Selectivity and response time of BD-diSeH (10 μM) towards sulfane sulfur over other RSS were examined in 10 mM HEPES (pH 7.4, 20% fetal bovine serum, v/v). As shown in Fig. 1d, five representative sulfane sulfurs including Na_2S_2, Na_2S_4, dibenzyl oligosulfane ($PhCH_2S_4CH_2Ph$), cysteine polysulfide and elemental sulfur (S_8) were selected as testing models. Once triggered by these sulfane sulfurs, BD-diSeH offered clear fluorescence increase within 1 min. In contrast, no fluorescence response was obtained within 4 min even under much higher concentrations of other RSS such as NaHS (100 μM), glutathione (GSH, 1 mM), cysteine (Cys, 500 μM), homocysteine (Hcys, 500 μM), cystine (Cys–Cys, 500 μM) and oxidized glutathione (GS–GS, 500 μM). Moreover, the reaction of probe BD-diSeH (10 μM) with Na_2S_4 (20 μM) at 37 °C yielded a time-dependent plot. Saturation of fluorescence intensity was obtained after incubation with Na_2S_4 for 80 s with 40-fold fluorescence increase (Fig. 1e). In addition, the probe showed high selectivity for sulfane sulfur even while coexisting with main biothiols at physiological concentrations (Fig. 1f). All these results demonstrated that BD-diSeH exhibited high selectivity and rapid response for sulfane sulfur.

MTT assay and photostability

The above successful results inspired us to apply our new fluorescent probe in biological systems. Before imaging sulfane sulfur in living cells, the cytotoxicity of BD-diSeH was tested in A549 cells *via* MTT assay. As shown in Fig. S2 (ESI†), almost 90% of cells survived after incubation with 5 μM BD-diSeH for 24 h. The cell viability was maintained at 85% after treatment with 10 μM BD-diSeH. The results indicated that BD-diSeH exhibited low cytotoxicity. The photostability of BD-diSeH was also investigated through time-dependent fluorescence measurements. The stable fluorescence intensity indicated that the probe BD-diSeH could be used for long-time cell imaging (Fig. S3, ESI†).

Imaging exogenous and endogenous sulfane sulfur in cells

The probe BD-diSeH was then applied for the detection of exogenous and endogenous sulfane sulfur in living cells. Cells (Fig. 2) were cultured with BD-diSeH for 15 min at 37 °C before image acquisition. A549 cells (Fig. 2a) showed weak intracellular fluorescence. *N*-Ethylmaleimide (NEM) can scavange intracellular endogenous RSS. Cells (Fig. 2b) pretreated with NEM exhibited nearly no fluorescence signal. These results illustrated that BD-diSeH could be used to detect endogenous sulfane sulfur in cells. The next group of cells was treated with Na_2S_4 (1 μM) for 15 min. Strong fluorescence in the cells was obtained (Fig. 2c). Our probe could detect exogenous sulfane sulfur in living cells. Additional studies were performed to verify whether our probe could be used to image sulfane sulfurs generated by the enzymes cystathionine γ-lyase (CSE) and 3-mercaptopyruvate sulfurtransferase (3-MST) in cells.[46] Intracellular CSE mRNA was overexpressed upon stimulation of lipopolysaccharide (LPS). *N*-Acetyl-L-cysteine (NAC) was utilized to stimulate the activity of 3-MST and to elevate the level of sulfane sulfur.[47,48] After exposing the cells (Fig. 2d) to LPS for 16 h, the fluorescence intensity increased. Other cells were incubated with NAC for 48 h, and strong fluorescence response was acquired (Fig. 2e). As control experiments, the cells were pretreated with a CSE inhibitor DL-propargylglycine (PAG, 1 mM) and 3-MST inhibitor α-ketoglutarate (6 mM) (Fig. 2f and g).[49] Then, the cells were treated as described in Fig. 2d and e. The fluorescence intensity of these cells was significantly reduced. These results demonstrated that the probe BD-diSeH could be used for imaging sulfane sulfur generated by enzymes CSE and 3-MST.

We then explored the levels of sulfane sulfur in different cell lines. Human neuroblastoma (SH-SY5Y) cells, mouse macrophage

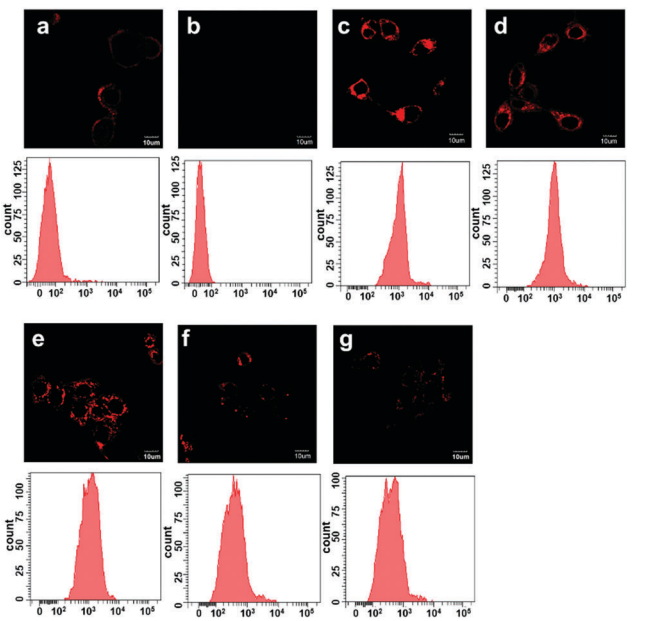

Fig. 2 Confocal microscopy images and flow cytometry analyses of A549 cells for the detection of sulfane sulfur using BD-diSeH. All cells were stained with BD-diSeH (1 μM) for 15 min and then imaged. (a) A549 cells were treated with BD-diSeH for 15 min at 37 °C; (b) cells incubated with 5 mM NEM for 30 min; (c) cells incubated with Na_2S_4 (1 μM) for 15 min at 37 °C; (d) A549 cells preincubated with LPS (1 μg mL^{-1}) for 16 h at 37 °C; (e) A549 cells preincubated with NAC (0.5 mM) for 48 h at 37 °C; (f) cells preincubated with DL-propargylglycine (PAG, 1 mM) and then treated with LPS (1 μg mL^{-1}) for 16 h at 37 °C; (g) cells pretreated with α-ketoglutarate (6 mM) and then treated with NAC (0.5 mM) for 48 h at 37 °C. Fluorescence collection windows were constructed from 680 to 780 nm for BD-diSeH. λ_{ex} = 635 nm.

264.7 (RAW 264.7) cells, human cervical carcinoma (Hela) cells, human embryonic kidney 293 (HEK 293) cells, human hepatocellular liver carcinoma (HepG2) cells, and human hepatocellular liver carcinoma (SMMC7721) cells were employed. The cells were first incubated with BD-diSeH (1 μM) for 15 min. Weak fluorescence intensities were observed, as shown in Fig. S4a–f. The results suggested that different cell lines held different concentrations of sulfane sulfur. After washing with PBS and further treatment with Na_2S_4 (1 μM) for another 15 min, as expected, strong fluorescence was observed in these cells, indicating that BD-diSeH could be employed to detect sulfane sulfur in different cell lines.

Influence on sulfane sulfur under hypoxic stress

Sulfane sulfur exhibits protective properties by scavenging free radicals and enhancing the activities of antioxidative enzymes such as glutathione peroxidase, glutathione reductase, and superoxide dismutase.[50–52] As is well-known, hypoxic stress can cause overproduction of oxygen radicals and lipid peroxides, which can inhibit the activity of antioxidant enzymes. Therefore, we attempted to trace the dynamic changes of sulfane sulfur using BD-diSeH in living cells under hypoxic condition. One assay was performed to examine the generation of sulfane sulfur under hypoxic condition at different time points using AnaeroPack (<0.1% O_2, 5% CO_2). There was a time-dependent increase in fluorescence intensity in A549 cells from 0 min to 180 min and decrease in the fluorescence intensity from 240 min to 380 min. However, during the time interval from 180 min to 240 min, the fluorescence intensity was saturated and maintained (Fig. 3a and b). Flow cytometry studies were consistent with imaging assays (Fig. 3c). Changes in sulfane sulfur levels could be due to self-protection of biological systems. These results indicated that our probe could work well in tracing dynamic endogenous sulfane sulfur changes under hypoxic stress.

Another assay was carried out to evaluate the production of sulfane sulfur under various oxygen concentrations. The probe BD-diSeH was loaded into A549 cells and incubated under various oxygen concentrations (20%, 10%, 5%, 1%, 0.1%) for 3 h. As shown in Fig. 4, the fluorescence intensity increased with decreased concentrations of oxygen. There was a strong increase in fluorescence intensity when the oxygen concentration was less than 1%. Flow cytometry studies were performed to further confirm these results. The result showed that fluorescence intensities of the cells were related to the degree of hypoxic stress. This generation of sulfane sulfur could play a significant role in protecting cells from oxidative damage induced by hypoxic stress.

In addition, subcellular location of BD-diSeH in A549 cells was investigated by co-staining with cytoplasm targetable dye Calcein-AM (5 μM, green channel) and nuclear fluorescence marker Hoechst 33342 (1 μg mL^{-1}, blue channel). The images merged well between BD-diSeH and Calcein-AM (Fig. 4 overlay), indicating preferential distribution of BD-diSeH in cytoplasm. Moreover, color-pair intensity correlation analysis showed a highly correlated plot between intensity distributions of BD-diSeH and Calcein-AM.

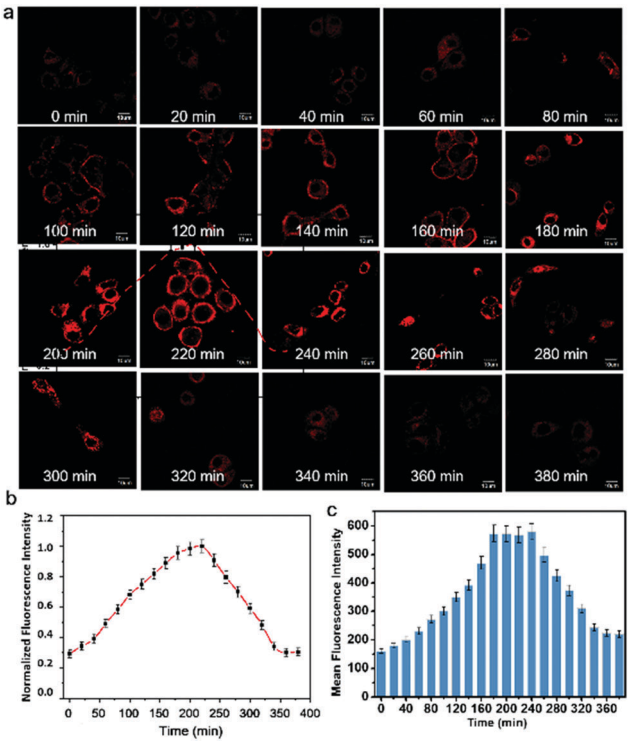

Fig. 3 (a) Fluorescence images of A549 cells using BD-diSeH at different time points of hypoxic condition. (b) Normalized fluorescence intensity of single cell in Fig. 3a (n = 8). (c) Mean fluorescence intensity of flow cytometry analysis for Fig. 3a. A549 cells were pre-incubated with BD-diSeH (1 μM) and then placed in an AnaeroPack. Fluorescence collection windows were constructed from 680 to 780 nm for BD-diSeH. λ_{ex} = 635 nm.

Imaging sulfane sulfur in 3D-multicellular spheroid

Having assessed the levels of sulfane sulfur in monolayer cells, we next attempted to evaluate the levels of sulfane sulfur in three-dimensional multicellular spheroids (3D-MCs), which were cultured in a non-adhesive environment. We proposed that 3D-MCs prohibited outside oxygen from entering, forming a hypoxic environment in the interior. SH-SY5Y cells with a diameter of 300 μm (Fig. 5) were selected to construct 3D-MCs. After treatment with BD-diSeH for 8 h under 20% O_2, 3D-MCs exhibited intense fluorescence emission only in their interior (z-axis: 50–150 μm), whereas the signal was quite weak in the periphery (z-axis: 0–50 μm). The images of Z-stack reconstruction for 3D-MCs exhibited that the fluorescence signals were activated at a depth of 150 μm, indicating that BD-diSeH could penetrate the interior for sulfane sulfur imaging (Fig. 5a). The 3D perspective images further verified that fluorescence was emitted from the interior rather than the external part (Fig. 5d). The quantitative and spatial distribution of fluorescence signal intensity of the yellow arrow in Fig. 5b is shown in Fig. 5c. The result indicated that the hypoxic interior of 3D-MCs induced overproduction of sulfane sulfur. Our probe was found to be capable of detecting sulfane sulfur changes in a hypoxic model.

Imaging sulfane sulfur in hypoxic brain

The brain occupies approximately 2–3% of the body's weight, and it consumes approximately 20% of the body's oxygen.

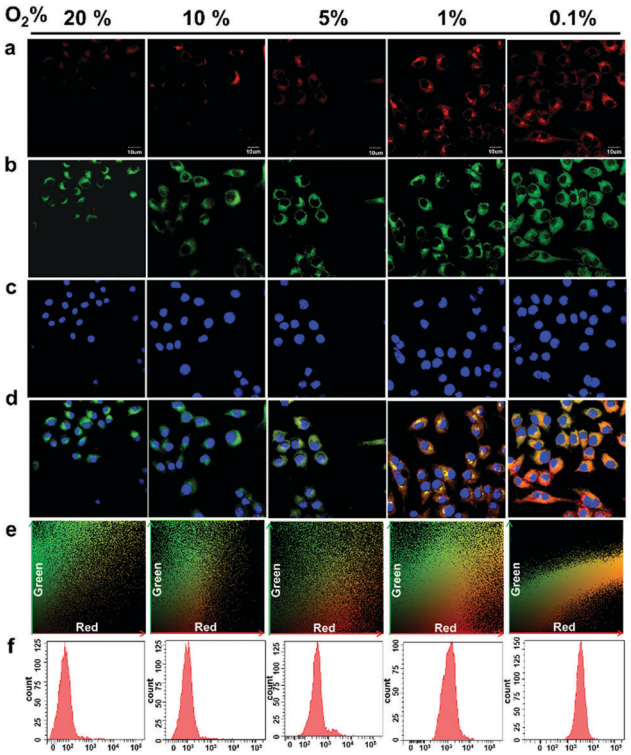

Fig. 4 Fluorescence images of A549 cells using BD-diSeH at different oxygen concentrations (20%, 10%, 5%, 1%, 0.1%). (a) A549 cells were incubated with BD-diSeH (1 μM) for 3 h under various oxygen concentrations. Then, the cells were further incubated with (b) Calcein-AM (5 μM) and (c) Hoechst 33342 (1 μg mL^{-1}) for 30 min. (d) Colocalization images of red, green and blue channels. (e) Correlation plot of red and green channels. (f) Flow cytometry assay of A549 cells using BD-diSeH at different oxygen concentrations (20%, 10%, 5%, 1%, 0.1%). Fluorescence collection windows constructed from 680 to 780 nm for BD-diSeH, 500 to 550 nm for Calcein-AM, and 425 to 500 nm for Hoechst 33342; λ_{ex} = 635, 488, and 405 nm, respectively.

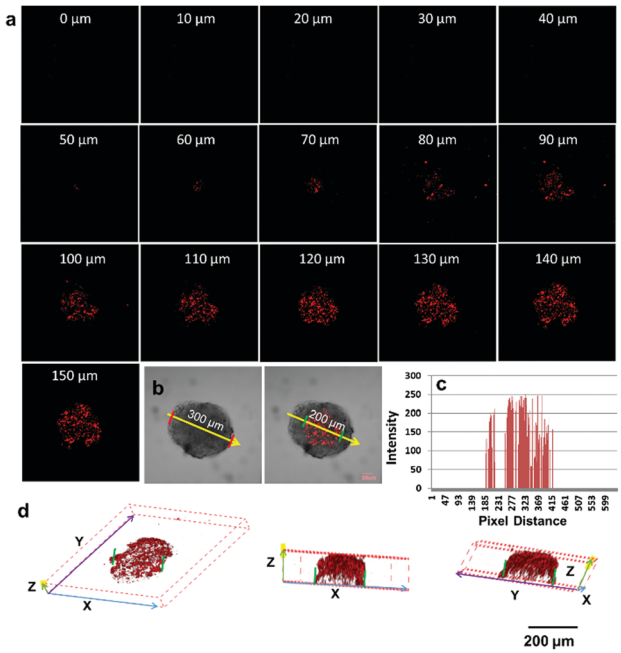

Fig. 5 (a) Fluorescence images of SH-SY5Y MCs upon incubation with BD-diSeH (1 μM) for 8 h at 37 °C. Images were acquired by Z-stack scan at 10 μm intervals. Fluorescence collection window was constructed from 680 to 780 nm. (b) Bright field image and overlay image. (c) Quantitative and spatial distribution of fluorescence signal intensity of the yellow arrow in figure b. (d) Different angles of MCs by Z-stack scan image reconstruction.

Therefore, it is very sensitive to hypoxia. Cerebral hypoxia leads to manifestation of neurological dysfunction and ultimately causes brain injury such as ischemic stroke[53] and Alzheimer's disease.[54] The brain possesses high sulfane sulfur levels to combat the overproduction of hypoxia-induced ROS. We explored the concentration changes of sulfane sulfur during cerebral hypoxia. BALB/c mice were placed in normobaric hypoxic chambers for 1–4 days to build hypoxic mouse models (fraction of inspiration O_2, FIO2 11%). After carefully isolating the hippocampus from sacrificed mice, hippocampus slices were stained with BD-diSeH for 20 min. The above experiments were performed in an anoxic glove box (11% O_2). As shown in Fig. 6a, a clear decrease in fluorescence intensity (1–3 days) was observed over hypoxic time, indicating that the levels of sulfane sulfur had decreased in the hippocampus (Fig. 6b). The results implied that hypoxia-induced ROS in the hippocampus can deplete most of the sulfane sulfur. However, we found that the body began its self-repair mechanism to increase the levels of sulfane sulfur on the 4th day. Hypoxia-inducible factor 1α (HIF-1α) is involved in response to low oxygen concentration in the cellular milieu and is expressed under hypoxia. The expression of HIF-1α was positively correlated with hypoxic time (Fig. 6c). These results indicated that our probe could be applied for sulfane sulfur imaging in the hippocampus under hypoxic condition, which could better clarify the changes in sulfane sulfur levels during hypoxic periods.

Imaging sulfane sulfur in mice

Near-infrared fluorescence is useful for deep imaging in organisms. To explore the capability of BD-diSeH for sulfane sulfur detection *in vivo*, BALB/c mice were selected as testing models for *in vivo* imaging using an *in vivo* imaging system. BALB/c mice (Fig. 6d) were divided into three groups. Mice in group a were injected intraperitoneally with BD-diSeH for 20 min as a control. In group b, mice were first pretreated with Na_2S_4 (20 μM, 50 μL in saline), followed by incubation with BD-diSeH for 20 min. The mice exhibited strong fluorescence increase. In group c, mice were given intraperitoneal (i.p.) cavity injection with LPS (10 μg mL^{-1}, 100 μL in 1 : 9 DMSO–saline, v/v) for 24 h to induce CSE mRNA overexpression.[55] As a CSE activator, pyridoxal-phosphate (PLP, 1 μM) was injected in i.p. cavity to improve the CSE activity and to promote the initial production rate of sulfane sulfur. Then, the mice were treated with BD-diSeH for 20 min prior to *in vivo* imaging. As expected, intense fluorescence emission was obtained in group c. The quantifications of mean fluorescence intensities for each group are shown in Fig. 6e. All results demonstrated that BD-diSeH could be applied to detect sulfane sulfur in living animals.

Imaging sulfane sulfur in hypoxic zebrafish

Hypoxia is a significant issue in aquatic systems. As a valuable vertebrate model organism, zebrafishes have been used

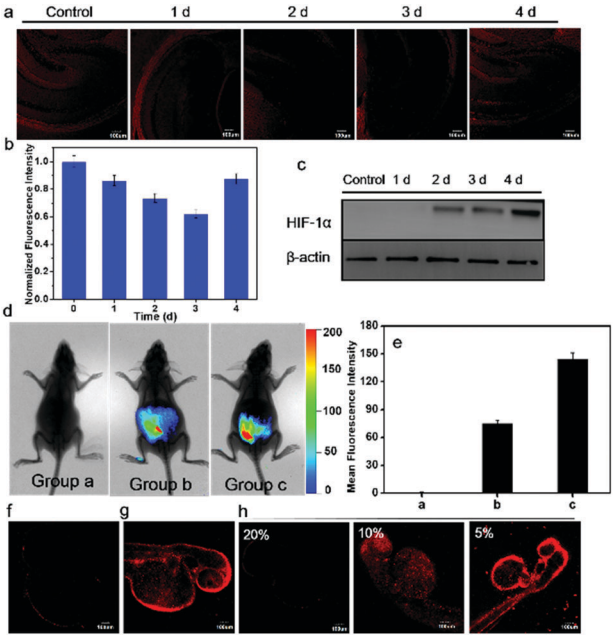

Fig. 6 (a) Confocal fluorescence images of hippocampus slice using BD-diSeH. Hippocampus slices were incubated with BD-diSeH (1 μM) for 20 min. λ_{ex} = 635 nm. Fluorescence collection window was constructed from 680 to 780 nm. (b) Normalized fluorescence intensity of Fig. 6a. Data are presented as means ± SD (n = 5). (c) Western blot analysis of HIF-1α β-actin was taken as loading control. (d) Fluorescence images of BALB/c mice visualizing sulfane sulfur level changes using BD-diSeH. Images represent emission intensities in collection window from 700 to 800 nm, λ_{ex} = 680 nm. Group a was injected i.p. with BD-diSeH (10 μM, 50 μL in 1 : 9 DMSO–saline, v/v) for 20 min. Group b was first pretreated with Na_2S_4 (20 μM, 50 μL in saline), then injected with BD-diSeH for 20 min. Group c was first injected with LPS (10 μg mL^{-1}, 100 μL in 1 : 9 DMSO–saline, v/v) for 24 h and PLP (1 μM, 50 μL in saline) for 2 h, then injected with BD-diSeH for 20 min. (e) Mean fluorescence intensities of groups a–c. The total number of photons from the entire peritoneal cavity of mice was integrated. Data are presented as means ± SD (n = 5). (f–h) Fluorescence images of zebrafish visualizing sulfane sulfur level changes using BD-diSeH. (f) Zebrafish was treated with BD-diSeH (1 μM) for 15 min. (g) Zebrafish was pretreated with Na_2S_4 (2 μM), then injected with BD-diSeH for 15 min. (h) Fluorescence images of zebrafish using BD-diSeH at different oxygen concentrations. Zebrafish was incubated with BD-diSeH (1 μM) for 1 h under various oxygen concentrations (20%, 10%, 5%).

in a variety of biological researches. We selected zebrafish as the research subject to investigate the effects of hypoxia on the expression of sulfane sulfur. Zebrafishes were loaded with BD-diSeH for 15 min before imaging. As shown in Fig. 6f, two-day-old zebrafish exhibited a weak fluorescence signal. After loading with Na_2S_4, zebrafish exhibited a strong fluorescence signal (Fig. 6g). The zebrafish treated under different oxygen levels from 20% to 5% for 1 h produced a gradual increase in fluorescence signal (Fig. 6h). The expressions of sulfane sulfur in hypoxic zebrafish increased, which may be ascribed to the physiological response against hypoxia. The released sulfane sulfur was likely to inhibit hypoxia-induced ROS elevation. These results revealed that this probe was suitable for imaging sulfane sulfur *in vivo* under hypoxic conditions.

Conclusions

In summary, we have rationally designed and synthesized a fluorescent probe BD-diSeH, which enables real-time imaging of endogenous and exogenous sulfane sulfur in living cells, 3D-multicellular spheroid, hippocampus, and *in vivo*. The probe BD-diSeH is composed of two moieties: the strong nucleophilic phenylselenol group (–SeH) is integrated into the NIR azo-BODIPY fluorophore *via* an ester bridge. BD-diSeH exhibits excellent selectivity and high sensitivity for the detection of sulfane sulfur. This newly developed probe can serve as an effective imaging tool for tracing endogenous sulfane sulfur changes under hypoxic stress. The relationship between the changes in sulfane sulfur levels and the degree and length of hypoxic stress has been investigated in cells, 3D-multicellular spheroids, and the hippocampus. The results presented here hold great promise for exploring the biological and physiological roles of endogenous sulfane sulfur in living systems.

Conflicts of interest

There are no conflicts to declare.

Acknowledgements

We thank the National Nature Science Foundation of China (No. 21775162, 41776110, and 21575159), the program of Youth Innovation Promotion Association, CAS (Grant 2015170), State Key Laboratory of Environmental Chemistry and Ecotoxicology, Research Center for Eco-Environmental Sciences, CAS (Grant KF2016-22), and the Key Laboratory of Sensor Analysis of Tumor Marker Ministry of Education, Qingdao University of Science and Technology (Grant SATM201705).

Notes and references

1 R. M. Yu, D. L. Chu, T. F. Tan, V. W. Li, A. K. Chan, J. P. Giesy, S. H. Cheng, R. S. Wu and R. Y. Kong, Leptin-mediated modulation of steroidogenic gene expression in hypoxic zebrafish embryos: implications for the disruption of sex steroids, *Environ. Sci. Technol.*, 2012, **46**, 9112–9119.

2 J. A. Fitzgerald, H. M. Jameson, V. H. Dewar Fowler, G. L. Bond, L. K. Bickley, T. M. Uren Webster, N. R. Bury, R. J. Wilson and E. M. Santos, Hypoxia suppressed copper toxicity during early development in zebrafish embryos in a process mediated by the activation of the HIF signaling pathway, *Environ. Sci. Technol.*, 2016, **50**, 4502–4512.

3 E. H. Shang and R. S. Wu, Aquatic hypoxia is a teratogen and affects fish embryonic development, *Environ. Sci. Technol.*, 2004, **38**, 4763–4767.

4 P. Nagyand and M. T. Ashby, Reactive sulfur species: kinetics and mechanisms of the oxidation of cysteine by hypohalous acid to give cysteine sulfenic acid, *J. Am. Chem. Soc.*, 2007, **129**(45), 14082–14091.

5 G. I. Giles and C. Jacob, Reactive sulfur species: an emerging concept in oxidative stress, *Biol. Chem.*, 2002, **383**(3–4), 375–388.

6 M. C. H. Gruhlke and A. J. Slusarenko, The biology of reactive sulfur species (RSS), *Plant Physiol. Biochem.*, 2012, **59**, 98–107.

7 H. S. Jung, X. Chen, J. S. Kim and J. Yoon, Recent progress in luminescent and colorimetric chemosensors for detection of thiols, *Chem. Soc. Rev.*, 2013, **42**(14), 6019–6031.

8 X. Zhang, J. Yin and J. Yoon, Recent advances in development of chiral fluorescent and colorimetric sensors, *Chem. Rev.*, 2014, **114**(9), 4918–4959.

9 K. Ono, T. Akaike, T. Sawa, Y. Kumagai, D. A. Wink, D. J. Tantillo, A. J. Hobbs, P. Nagy, M. Xian, J. Lin and J. M. Fukuto, Redox chemistry and chemical biology of H_2S, hydropersulfides, and derived species: implications of their possible biological activity and utility, *Free Radical Biol. Med.*, 2014, **77**, 82–94.

10 J. I. Toohey and A. J. L. Cooper, Thiosulfoxide (sulfane) sulfur: new chemistry and new regulatory roles in biology, *Molecules*, 2014, **19**(8), 12789–12813.

11 G. Roos and J. Messens, Protein sulfenic acid formation: from cellular damage to redox regulation, *Free Radical Biol. Med.*, 2011, **51**(2), 314–326.

12 S. Laxman, B. M. Sutter, X. Wu, S. Kumar, X. Guo, D. C. Trudgian, H. Mirzaei and B. P. Tu, Sulfur amino acids regulate translational capacity and metabolic homeostasis through modulation of tRNA thiolation, *Cell*, 2013, **154**(2), 416–429.

13 J. L. Wood, Sulfane sulfur, *Methods Enzymol.*, 1987, **143**, 25–29.

14 T. Ueno and T. Nagano, Fluorescent probes for sensing and imaging, *Nat. Methods*, 2011, **8**(8), 642–645.

15 X. Li, X. Gao, W. Shi and H. Ma, Design strategies for water-soluble small molecular chromogenic and fluorogenic probes, *Chem. Rev.*, 2014, **114**(1), 590–659.

16 H. Liu, K. Li, X. Hu, L. Zhu, Q. Rong, Y. Liu, X. Zhang, J. Hasserodt, F. Qu and W. Tan, *In situ* localization of enzyme activity in live cells by a molecular probe releasing a precipitating fluorochrome, *Angew. Chem., Int. Ed.*, 2017, **56**, 11788–11792.

17 H. Liu, Y. Liu, P. Wang and X. Zhang, Molecular engineering of two-photon fluorescent probes for bioimaging applications, *Methods Appl. Fluoresc.*, 2017, **5**, 012003.

18 Z. Han, X. Zhang, L. Qiao, C. Li, L. Jian, G. Shen and R. Yu, Efficient Fluorescence Resonance Energy Transfer-Based Ratiometric Fluorescent Cellular Imaging Probe for Zn^{2+} Using a Rhodamine Spirolactam as a Trigger, *Anal. Chem.*, 2010, **82**, 3108–3113.

19 X. Chen, F. Wang, J. Y. Hyun, T. Wei, J. Qiang, X. Ren, I. Shin and J. Yoon, Recent progress in the development of fluorescent, luminescent and colorimetric probes for detection of reactive oxygen and nitrogen species, *Chem. Soc. Rev.*, 2016, **45**(10), 2976–3016.

20 V. S. Lin, W. Chen, M. Xian and C. J. Chang, Chemical probes for molecular imaging and detection of hydrogen sulfide and reactive sulfur species in biological systems, *Chem. Soc. Rev.*, 2015, **44**(14), 4596–4618.

21 Y. Takano, K. Shimamoto and K. Hanaoka, Chemical tools for the study of hydrogen sulfide (H_2S) and sulfane sulfur and their applications to biological studies, *J. Clin. Biochem. Nutr.*, 2016, **58**(1), 7–15.

22 G. Mao, T. Wei, X. Wang, S. Huan, D. Lu, J. Zhang, X. Zhang, W. Tan, G. Shen and R. Yu, High-Sensitivity Naphthalene-Based Two-Photon Fluorescent Probe Suitable for Direct Bioimaging of H_2S in Living Cells, *Anal. Chem.*, 2013, **85**, 7875–7881.

23 Y. Takano, K. Hanaoka, K. Shimamoto, R. Miyamoto, T. Komatsu, T. Ueno, T. Terai, H. Kimura, T. Nagano and Y. Urano, Development of a reversible fluorescent probe for reactive sulfur species, sulfane sulfur, and its biological application, *Chem. Commun.*, 2017, **53**(6), 1064–1067.

24 M. Ikeda, Y. Ishima, A. Shibata, V. T. G. Chuang, T. Sawa, H. Ihara, H. Watanabe, M. Xian, Y. Ouchi, T. Shimizu, H. Ando, M. Ukawa, T. Ishida, T. Akaike, M. Otagiri and T. Maruyama, Quantitative determination of polysulfide in albumins, plasma proteins and biological fluid samples using a novel combined assays approach, *Anal. Chim. Acta*, 2017, **969**, 18–25.

25 W. Chen, C. Liu, B. Peng, Y. Zhao, A. Pacheco and M. Xian, New fluorescent probes for sulfane sulfurs and the application in bioimaging, *Chem. Sci.*, 2013, **4**(7), 2892–2896.

26 X. Han, X. Song, B. Li, F. Yu and L. Chen, A near-infrared fluorescent probe for sensitive detection and imaging of sulfane sulfur in living cells and *in vivo*, *Biomater. Sci.*, 2018, **6**(3), 672–682.

27 M. Gao, R. Wang, F. Yu, J. You and L. Chen, Imaging and evaluation of sulfane sulfur in acute brain ischemia using a mitochondria-targeted near-infrared fluorescent probe, *J. Mater. Chem. B*, 2018, **6**, 2608–2619.

28 F. Yu, M. Gao, M. Li and L. Chen, A dual response near-infrared fluorescent probe for hydrogen polysulfides and superoxide anion detection in cells and *in vivo*, *Biomaterials*, 2015, **63**, 93–101.

29 M. Gao, F. Yu, H. Chen and L. Chen, Near-infrared fluorescent probe for imaging mitochondrial hydrogen polysulfides in living cells and *in vivo*, *Anal. Chem.*, 2015, **87**(7), 3631–3638.

30 W. Chen, E. W. Rosser, T. Matsunaga, A. Pacheco, T. Akaike and M. Xian, The Development of fluorescent probes for visualizing intracellular hydrogen polysulfides, *Angew. Chem., Int. Ed.*, 2015, **54**(47), 13961–13965.

31 W. Chen, E. W. Rosser, D. Zhang, W. Shi, Y. Li, W. J. Dong, H. Ma, D. Hu and M. Xian, A specific nucleophilic ring-opening reaction of aziridines as a unique platform for the construction of hydrogen polysulfides sensors, *Org. Lett.*, 2015, **17**(11), 2776–2779.

32 M. Gao, R. Wang, F. Yu, J. You and L. Chen, A near-infrared fluorescent probe for the detection of hydrogen polysulfides biosynthetic pathways in living cells and *in vivo*, *Analyst*, 2015, **140**(11), 3766–3772.

33 Y. Huang, F. Yu, J. Wang and L. Chen, Near-infrared fluorescence probe for *in situ* detection of superoxide anion

and hydrogen polysulfides in mitochondrial oxidative stress, *Anal. Chem.*, 2016, **88**(7), 4122–4129.
34 L. Zeng, S. Chen, T. Xia, W. Hu, C. Li and Z. Liu, Two-photon fluorescent probe for detection of exogenous and endogenous hydrogen persulfide and polysulfide in living organisms, *Anal. Chem.*, 2015, **87**(5), 3004–3010.
35 C. Liu, W. Chen, W. Shi, B. Peng, Y. Zhao, H. Ma and M. Xian, Rational design and bioimaging applications of highly selective fluorescence probes for hydrogen polysulfides, *J. Am. Chem. Soc.*, 2014, **136**(20), 7257–7260.
36 W. Chen, A. Pacheco, Y. Takano, J. J. Day, K. Hanaoka and M. Xian, A single fluorescent probe to visualize hydrogen sulfide and hydrogen polysulfides with different fluorescence signals, *Angew. Chem., Int. Ed.*, 2016, **55**(34), 9993–9996.
37 H. Shang, H. Chen, Y. Tang, R. Guo and W. Lin, Construction of a two-photon fluorescent turn-on probe for hydrogen persulfide and polysulfide and its bioimaging application in living mice, *Sens. Actuators, B*, 2016, **230**, 773–778.
38 Q. Han, Z. Mou, H. Wang, X. Tang, Z. Dong, L. Wang, X. Dong and W. Liu, Highly selective and sensitive one- and two-photon ratiometric fluorescent probe for intracellular hydrogen polysulfide sensing, *Anal. Chem.*, 2016, **88**(14), 7206–7212.
39 X. Han, F. Yu, X. Song and L. Chen, Quantification of cysteine hydropersulfide with a ratiometric near-infrared fluorescent probe based on selenium-sulfur exchange reaction, *Chem. Sci.*, 2016, **7**(8), 5098–5107.
40 S. A. Hilderbrand and R. Weissleder, Near-infrared fluorescence: application to *in vivo* molecular imaging, *Curr. Opin. Chem. Biol.*, 2010, **14**(1), 71–79.
41 J. V. Frangioni, *In vivo* near-infrared fluorescence imaging, *Curr. Opin. Chem. Biol.*, 2003, **7**(5), 626–634.
42 H. Zhang, J. Liu, L. Wang, M. Sun, X. Yan, J. Wang, J. P. Guo and W. Guo, Amino-Si-rhodamines: a new class of two-photon fluorescent dyes with intrinsic targeting ability for lysosomes, *Biomaterials*, 2018, **158**, 10–22.
43 Y. Q. Sun, J. Liu, H. Zhang, Y. Huo, X. Lv, Y. Shi and W. Guo, A mitochondria-targetable fluorescent probe for dual-channel no imaging assisted by intracellular cysteine and glutathione, *J. Am. Chem. Soc.*, 2014, **136**(36), 12520–12523.
44 N. Boens, V. Leen and W. Dehaen, Fluorescent indicators based on BODIPY, *Chem. Soc. Rev.*, 2012, **41**(3), 1130–1172.
45 M. Gao, R. Wang, F. Yu and L. Chen, Evaluation of sulfane sulfur bioeffects *via* a mitochondria-targeting selenium-containing near-infrared fluorescent probe, *Biomaterials*, 2018, **160**, 1–14.
46 T. Ida, T. Sawa, H. Ihara, Y. Tsuchiya, Y. Watanabe, Y. Kumagai, M. Suematsu, H. Motohashi, S. Fujii, T. Matsunaga, M. Yamamoto, K. Ono, N. O. Devarie-Baez, M. Xian, J. M. Fukuto and T. Akaike, Reactive cysteine persulfides and *S*-polythiolation regulate oxidative stress and redox signaling, *Proc. Natl. Acad. Sci. U. S. A.*, 2014, **111**(21), 7606–7611.
47 H. Jurkowska, W. Placha, N. Nagahara and M. Wróbel, The expression and activity of cystathionine-γ-lyase and 3-mercaptopyruvate sulfurtransferase in human neoplastic cell lines, *Amino Acids*, 2011, **41**(1), 151–158.
48 H. Jurkowska and M. Wróbel, *N*-Acetyl-L-cysteine as a source of sulfane sulfur in astrocytoma and astrocyte cultures: correlations with cell proliferation, *Amino Acids*, 2008, **34**(2), 231–237.
49 V. S. Lin, A. R. Lippert and C. J. Chang, Cell-trappable fluorescent probes for endogenous hydrogen sulfide signaling and imaging H_2O_2-dependent H_2S production, *Proc. Natl. Acad. Sci. U. S. A.*, 2013, **110**(18), 7131–7135.
50 M. Iciek and L. Wlodek, Biosynthesis and biological properties of compounds containing highly reactive, reduced sulfane sulfur, *Pol. J. Pharmacol.*, 2001, **53**(3), 215–225.
51 J. I. Toohey, Persulfide sulfur is a growth-factor for cells defective in sulfur metabolism, *Biochem. Cell Biol.*, 1986, **64**(8), 758–765.
52 L. Y. Sheen, H. W. Chen, Y. L. Kung, C. T. Liu and C. K. Lii, Effects of garlic oil and its organosulfur compounds on the activities of hepatic drug-metabolizing and antioxidant enzymes in rats fed high- and low-fat diets, *Nutr. Cancer*, 1999, **35**(2), 160–166.
53 C. Roffe, Hypoxia and stroke, *Age Ageing*, 2002, **31**, 10–13.
54 C. Peers, H. A. Pearson and J. P. Boyle, Hypoxia and Alzheimer's disease, *Essays Biochem.*, 2007, **43**, 153–164.
55 X. Y. Zhu, S. J. Liu, Y. J. Liu, S. Wang and X. Ni, Glucocorticoids suppress cystathionine gamma-lyase expression and H_2S production in lipopolysaccharide-treated macrophages, *Cell. Mol. Life Sci.*, 2010, **67**(7), 1119–1132.